Effects of Ethanol Addition on n-Heptane Decomposition in Premixed Flames

ARTICLE *in* ENERGY & FUELS · NOVEMBER 2008

Impact Factor: 2.79 · DOI: 10.1021/ef800519s

4 AUTHORS, INCLUDING:

Chunde Yao
Tianjin University
138 PUBLICATIONS **772** CITATIONS

SEE PROFILE

Effects of Ethanol Addition on *n*-Heptane Decomposition in Premixed Flames

Jinou Song,* Chunde Yao, Shiyu Liu, and Hanjun Xu

State Key Laboratory of Engines, Tianjin University, Tianjin 300072, China

Received June 30, 2008. Revised Manuscript Received September 21, 2008

The goal of this paper is to explain the effects of ethanol addition on *n*-heptane decomposition and partial oxidation processes. An experimental study of the oxidation of *n*-heptane in the absence and presence of ethanol has been performed. The specific flames were low-pressure (25 Torr), laminar, premixed flames at an equivalence ratio of 1.0. The experiment was performed with tunable synchrotron vacuum ultraviolet (VUV) photoionization and molecular-beam mass spectrometry. Major species on the centerline of each flame were identified by measurements of the photoionization mass spectrum and photoionization efficiency (PIE) spectra. Mole fraction profiles of these species were derived at the selected photon energies near the ionization thresholds. With the addition of ethanol, the partial oxidation of *n*-heptane into ketones was enhanced and 1-butene mainly decomposed to 1,3-butadiyne instead of 1,3-butadiene. Propargyl radicals were more important than butenynyl and butadienyl radicals in benzene formation.

1. Introduction

n-Heptane is a component of commercial gasoline and one of the primary reference fuels for the determination of the gasoline octane number. The combustion research community has endeavored to develop detailed chemical kinetic mechanisms for the combustion of *n*-heptane. The oxidation of *n*-heptane has been investigated in shock tubes,[1] jet-stirred reactors,[2] and premixed[3,4] and diffusion[5] flames. The ignition of *n*-heptane/oxygen/Ar mixtures behind incident and reflected shock waves has been studied by Coats and Williams.[6] Temperature and species (stable and free radicals) mole fraction profiles in laminar, premixed *n*-heptane/oxygen/argon flames have been obtained by Doute et al.[3] Recently, McEnally et al.[7] have studied fuel decomposition and hydrocarbon growth processes in a premixed *n*-heptane flame. Temperature and species measurements were reported, and polycyclic aromatic hydrocarbon (PAH) growth mechanisms were analyzed in the study.

For the sake of the improvement in motor vehicle fuel properties, fuel oxygenates were first used as an octane replacement for lead because lead inactivates the exhaust catalyst. They are also known for their ability to reduce exhaust CO emissions by leaning the fuel−air mixture.[8] Several oxygen-containing compounds (i.e., oxygenates), such as alcohols (e.g., methanol, ethanol, and tertiary butyl alcohol) and ethers [e.g., methyl tertiary butyl ether (MTBE), ethyl tertiary butyl ether (ETBE), and tertiary amyl methyl ether (TAME)] were considered as the most common fuel oxygenates. The use of ethers is in decline because of their effect on groundwater.

Inal and Senkan[9,10] have studied the effect of the addition of three fuel oxygenates (methanol, ethanol, and MTBE) on the formation of PAHs and soot and reported the species mole fraction and temperature profiles in laminar, premixed, atmospheric pressure, fuel-rich flames of *n*-heptane. Several previous studies also focused on the effect of oxygenate addition on the combustion in engines.[11−13] The effects of blending unleaded gasoline with different proportions of oxygenate on exhaust carbon monoxide, carbon dioxide, and hydrocarbon emissions from a fixed compression ratio spark-ignition (SI) engine were reported.

Understanding the combustion mechanism of *n*-heptane flame with oxygenated additives needs the comprehensive identification and concentration measurement of the initial heptane decomposition and oxidation products, which were scarcely investigated in previous studies. With tunable synchrotron vacuum ultraviolet (VUV) photoionization and molecular-beam sampling mass spectrometry, this paper studied premixed, laminar, low-pressure (25 Torr) flames of *n*-heptane/oxygen/argon and *n*-heptane/ethanol/oxygen/argon. The goals of the research were to report experimental investigation on heptane combustion and to gain additional understanding of the effects of ethanol on heptane oxidation kinetics.

2. Experimental Section

The experiment was performed at the combustion endstation of the National Synchrotron Radiation Laboratory (NSRL), University

* To whom correspondence should be addressed. E-mail: songjinou@tju.edu.cn.

(1) Ciezki, H.; Adomeit, G. *Int. Symp. Shock Tubes Waves* **1987**, *16*, 481–486.
(2) Dagaut, P.; Reuillon, M.; Cathonnet, M. *Combust. Flame* **1995**, *101*, 132–140.
(3) Doute, C.; Delfau, J. L.; Akrich, R.; Vovelle, C. *Combust. Sci. Technol.* **1997**, *124*, 249–276.
(4) Ingemarsson, A. T.; Pedersen, J. R.; Olsson, J. O. *J. Phys. Chem. A* **1999**, *103*, 8222–8230.
(5) Peterca, L.; Marconi, F. *Combust. Flame* **1989**, *78*, 308–325.
(6) Coats, C. M.; Williams, A. *Proc. Combust. Inst.* **1979**, *17*, 611–621.
(7) McEnally, C. S.; Ciuparu, D. M.; Pfefferle, L. D. *Combust. Flame* **2003**, *134*, 339–353.
(8) Farhad, N.; Peter, Z.; George, E. H.; Shili, L. *Energy Policy* **2001**, *29*, 1–5.
(9) Inal, F.; Senkan, S. M. *Combust. Flame* **2002**, *131*, 16–28.
(10) Inal, F.; Senkan, S. M. *Fuel* **2005**, *84*, 495–503.
(11) Zervas, E.; Montagne, X.; Lahaye, J. *Fuel* **2005**, *83*, 2301–2311.
(12) Zervas, E.; Montagne, X.; Lahaye, J. *Fuel* **2004**, *83*, 2313–2321.
(13) Cadle, S. H.; Mulawa, P.; Groblicki, P.; Laroo, C.; Ragazzi, R. A.; Nelson, K.; Gallagher, G.; Zielinska, B. *Environ. Sci. Technol.* **2001**, *l35*, 26–32.

10.1021/ef800519s CCC: $40.75
Published on Web 11/19/2008

Table 1. Experimental Conditions (Equivalence Ratio, 1.0; Pressure, 25 Torr; Reactants Temperature, 200 °C)

	flame A	flame B
mixture	$C_7H_{16}/O_2/Ar$	$C_7H_{16}/C_2H_5OH/O_2/Ar$
flow rates (slm)[a]	0.092/1.0/0.8	0.065/0.12/1.0/0.8
n-heptane (mol %)	4.832	3.242
ethanol (mol %)	0	6.983

[a] slm is the abbreviation of liters per minute at standard ambient condition.

of Science and Technology of China. A detailed description of the instrument has been published elsewhere;[14] therefore, only a brief description will be given here. The apparatus consists of a flat burner situated in the flame chamber, a differentially pumped flame sampling system, and a photoionization chamber with a reflectron time-of-flight mass spectrometer (RTOFMS). A low-pressure laminar premixed flame on a 6.0 cm diameter flat burner (McKenna, U.S.A.) is sampled through a quartz nozzle with an orifice diameter of ~500 μm. The sampled gas forms a molecular beam, which passes into a differentially pumped ionization region, where it is crossed by the tunable synchrotron light.

The photoions are collected and analyzed by a RTOFMS with the mass resolving power ($m/\Delta m$) of ~1400. Movement of the burner toward or away from the quartz nozzle allows the mass spectrum to be taken at different positions in the flame. The ion signal is recorded using a multiscaler (FAST Comtec P7888, Germany), with a bin width of 2 ns. A DG535 is used to trigger the multiscaler and a pulsed power supply.

The ion signals, measured as a function of the photon energy and normalized by the photon flux, yield the photoionization efficiency (PIE) spectra, which can help identify combustion intermediates, including isomers and radicals. To avoid fragmentation and keep near-threshold photoionization, the burner was scanned at selected photon energies: 16.50, 11.80, 10.87, 10.00, 9.54, 9.00, and 8.49 eV. The mole fractions of these species were derived according to the method described by Cool et al.[15] The mole fractions have an uncertainty of ±25% for the stable intermediates and a factor of 2 for radicals. A Pt/Pt−13% Rh thermocouple with a diameter of 0.076 mm, coated with Y_2O_3−BeO antioxidant, was used to measure the flame temperature. The flame temperatures have an estimated uncertainty of about ±100 K.

The experimental conditions are listed in Table 1. Oxygen (99.99%) and argon (99%) were obtained from Nanjing Special Gas (China). *n*-Heptane (97%) and ethanol (HPLC grade, 99.7%) were obtained from China Pharmaceutical Group. The flow rates of oxygen and argon were controlled by calibrated mass flow controllers (Multi Gas Controller 647C, MKS). A syringe pump (ISCO 1000D USA) was used to introduce *n*-heptane or a *n*-heptane/ethanol blend into a vaporizer, with the temperature kept at 200 °C. In the following section, *n*-heptane flame is called flame A and *n*-heptane/ethanol flame is called flame B.

3. Results and Discussion

In this study, most attention is paid to the intermediates formed in *n*-heptane decomposition and hydrocarbon growth processes. Furthermore, flame temperature (T_g) and mole fractions of major species were also measured. The data are plotted against the height above the burner (Z). All measurements were performed on the burner centerline, and extracting gas samples began from the position of $Z = 1.5$ mm.

Flames A and B had similar temperature profiles (Figure 1) under the experimental conditions listed in Table 1. Therefore, the differences in intermediate concentrations can be mainly attributed to the effect of ethanol addition.

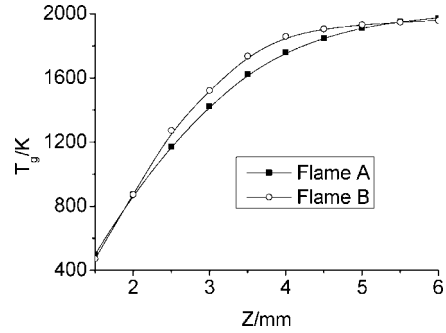

Figure 1. Temperature profiles of flames A and B.

Table 2. List of Species Measured in the Reaction Zone

			ionization energies (eV)		maximum mole fraction	
m/e	species	formula	experiment[a]	literature[b]	flame A	flame B
15	methyl radical	CH_3	9.84	9.84	6.8×10^{-3}	5.3×10^{-3}
28	ethylene	C_2H_4	10.54	10.51	9.5×10^{-3}	1.4×10^{-2}
29	ethyl radical	C_2H_5	8.39	8.26	7.3×10^{-4}	4.4×10^{-4}
40	propyne	C_3H_4	10.37	10.36	5.8×10^{-4}	2.0×10^{-4}
41[c]	allyl radical	C_3H_5	8.15	8.13	5.3×10^{-4}	
42	ketene	C_2H_2O	9.65	9.62	5.9×10^{-3}	3.5×10^{-3}
44	acetaldehyde	C_2H_4O	10.23	10.23	9.1×10^{-4}	5.18×10^{-3}
44	ethenol	C_2H_4O	9.34	9.33		3.3×10^{-4}
46	ethanol	C_2H_6O	10.50	10.48		1.2×10^{-2}
50	1,3-butadiyne	C_4H_2	10.20	10.17		8.6×10^{-4}
52	1-buten-3-yne	C_4H_4	9.61	9.58	9.4×10^{-5}	6.4×10^{-5}
54	1,3-butadiene	C_4H_6	9.08	9.07	1.4×10^{-3}	
54	1-butyne	C_4H_6	10.18	10.18	1.2×10^{-3}	6.4×10^{-4}
56	2-butene, (*E*)-	C_4H_8	9.08	9.10	3.1×10^{-4}	
56	1-butene	C_4H_8	9.63	9.55	1.9×10^{-3}	1.2×10^{-3}
58	acetone	C_3H_6O	9.70	9.70	1.6×10^{-4}	1.8×10^{-4}
60	ethane, methoxy-	C_3H_8O	9.78	9.72		5.3×10^{-5}
66	1,3-cyclopentadiene	C_5H_6	8.58	8.57	6.7×10^{-5}	3.8×10^{-5}
68	1,3-butadiene, 2-methyl	C_5H_8	8.83	8.86		
68	1,3-pentadiene, (*Z*)-	C_5H_8	8.64	8.62	1.4×10^{-4}	3.3×10^{-5}
70	1-pentene	C_5H_{10}	9.52	9.49	1.99×10^{-3}	1.14×10^{-3}
70	2-pentene, (*E*)-	C_5H_{10}	9.06	9.04	2.8×10^{-4}	1.6×10^{-4}
72	2-butanone	C_4H_8O	9.47	9.52	4.1×10^{-4}	3.1×10^{-4}
74	propane, 2-methoxy	$C_4H_{10}O$	9.41	9.45		4.1×10^{-4}
74	triacetylene	C_6H_2		9.48		
78	benzene	C_6H_6	9.25	9.24	2.4×10^{-5}	1.7×10^{-5}
80	1,3-cyclohexadiene	C_6H_8	8.27	8.25		2.8×10^{-5}
82	furan, 2-methyl-	C_5H_6O	8.37	8.38		6.9×10^{-5}
84	1-hexene	C_6H_{12}	9.45	9.44	8.5×10^{-4}	5.4×10^{-4}
86	2-pentanone	$C_5H_{10}O$	9.34	9.38		1.1×10^{-4}
92	toluene	C_7H_8	8.87	8.83		4.9×10^{-6}
100	heptane	C_7H_{16}	10.08	10.08	2.4×10^{-2}	1.5×10^{-2}
114	3-heptanone	$C_7H_{14}O$	9.17	9.15	2.8×10^{-4}	2.2×10^{-4}

[a] The experimental error for IEs is ±0.05 eV (see ref 16). [b] Refer to ref 25. [c] Mass 41 is determined to be C_2HO and C_3H_5 in flame A by the DER method and is determined only to be C_3H_5 in flame B by the PI method, which cannot detect C_2HO. C_2HO is very active and hardly detected; therefore the table only lists mass 41 as C_3H_5.

This paper focuses on the reaction zone, primarily interested in initial decomposition, large growth products, and oxygenates, which are listed in Table 2. The noise levels and background signals are small compared to the measured signals, even for benzene, which has a peak mole fraction of only 16 ppm in flame B (Figure 2).

Although detailed modeling is necessary to identify specific reaction pathways, the experimental results do provide some general insights into the formation mechanisms of these intermediates.

3.1. Mole Fraction Profiles of Ketones. The partial oxidation of heptane to oxygen-containing intermediates at temper-

(14) Qi, F.; Yang, R.; Yang, B.; Huang, C.; Wei, L.; Wang, J.; Sheng, L.; Zhang, Y. *Rev. Sci. Instrum.* **2006**, *77*, 084101.

(15) Cool, T. A.; Nakajima, K.; Taatjes, C. A.; McIlroy, A.; Westmoreland, P. R.; Law, M. E.; Morel, A. *Proc. Combust. Inst.* **2005**, *30*, 1681–1688.

(16) Huang, C.; Wei, L.; Yang, B.; Wang, J.; Li, Y.; Sheng, L.; Zhang, Y.; Qi, F. *Energy Fuels* **2006**, *20*, 1505–1513.

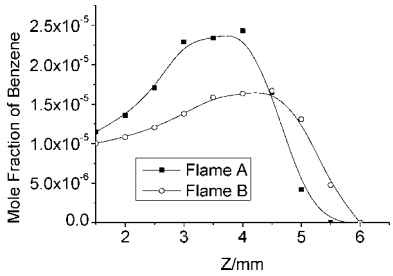

Figure 2. Profiles of benzene in flames A and B.

ature from ambient to 550 K has been studied at the presence of the catalysts.[17,18] A proposed mechanism for the oxidation of alkanes led to the formation of an alcohol intermediate, which in turn oxidized to an aldehyde or a ketone.[19] The resulting aldehydes and ketones can be oxidized to acids by the reaction with OH and O_2.[20]

Most researchers studying oxidation of heptane in combustors are primarily interested in heptane decomposition and hydrocarbon growth processes. However, few studies have been carried out on partial oxidation. The partial oxidation was observed in the heptane decomposition processes in the present experiment.

As shown in Table 1, the mole fraction of *n*-heptane in flame A is higher than in flame B but less ketones are formed in flame A and ketones in flame A peak at a higher height (Figures 7 and 8). These observations indicate that ethanol enhanced the partial oxidation of *n*-heptane.

3.2. Mole Fraction Profiles of the Hydrocarbon Intermediates. Figures 9 and 10 show the peak positions of major hydrocarbon intermediates. It can be observed that the consumption routes for heptane shifted with the ethanol addition.

1-Pentene peaked closer to the burner surface than 1-hexene in flame A (Figure 9) but further than 1-hexene in flame B (Figure 10). This observation indicates that *n*-heptane decomposed more toward 1-hexene in flame B than in flame A. Because the maximum mole fractions of 1-pentene were 2 times larger than those of 1-hexene in both flames (Figures 5 and 6), *n*-heptane decomposed to 1-pentene more predominantly than to 1-hexene.

1-Butene peaked at a higher height than 1-pentene in flame A (Figure 9) and at a slightly lower height than 1-pentene in flame B (Figures 6 and 10), which indicates that *n*-heptane decomposed more toward 1-butene in flame B than in flame A. 1-Butene decomposed to 1-butyne and 1,3-butandiene in flame A but to 1-butyne and 1,3-butandlyne in flame B.

Benzene formation is a critical step to soot production and has been studied extensively.[21] In this work, the peak positions of benzene related to the peak positions of propyne and 1-buten-3yne (Figures 2−4), which implicates that the candidates of the dominant benzene/phenyl formation pathways are reactions involving propargyl (C_3H_3),[22,23] butenynyl (n-C_4H_3), and butadienyl radicals (n-C_4H_5).[24]

Although the maximum mole fraction of 1,3-butadiyne was 4 times larger than that of propyne in flame B, the peak position of benzene is still closer to the peak position of propyne (Figures 2 and 4). This observation implies that butenynyl radicals (n-C_4H_3), even butadienyl radicals (n-C_4H_5), are less important than propargyl radicals (C_3H_3) in benzene formation.

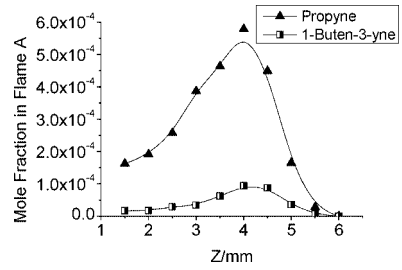

Figure 3. Profiles of benzene precursors in flame A.

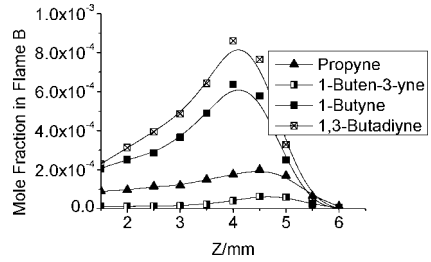

Figure 4. Profiles of benzene precursors in flame B.

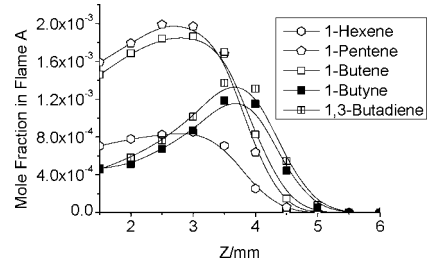

Figure 5. Profiles of major species mole fractions in flame A.

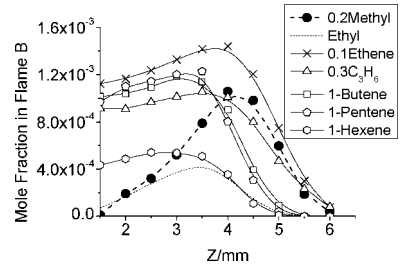

Figure 6. Profiles of major species mole fractions in flame B. Coordinate readings = [methyl] × 0.2 for methyl. Coordinate readings = [ethyl] × 0.1 for ethyl. Coordinate readings = [C_3H_6] × 0.3 for C_3H_6.

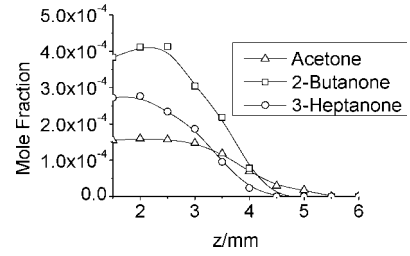

Figure 7. Profiles of major ketone mole fractions in flame A.

4. Concluding Remarks

Practical fuels generally blend oxygenates to improve motor vehicle fuel properties; thus, soot formation models should be

(17) Shang, J.; Du, Y.; Xu, Z. *Chemosphere* **2002**, *46*, 93–99.
(18) Stoylkova, T. Yu.; Chanev, Chr. D.; Lechert, H. T.; Bezouhanova, C. P. *Appl. Catal., A* **2000**, *203*, 121–126.
(19) Djeghri, N.; Teichner, S. J. *J. Catal.* **1980**, *62*, 99–106.
(20) Sopyan, I.; Murasawa, S. *Chem. Lett.* **1994**, *4*, 723–726.
(21) Richter, H.; Howard, J. B. *Prog. Energy Combust. Sci.* **2000**, *26*, 565–608.
(22) Pope, C. J.; Miller, J. A. *Proc. Combust. Inst.* **2000**, *28*, 1519–1527.

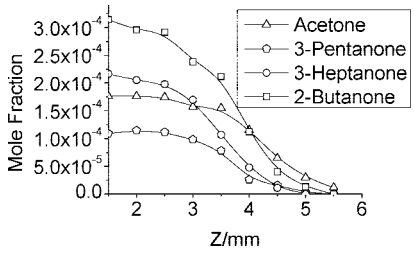

Figure 8. Profiles of major ketone mole fractions in flame B.

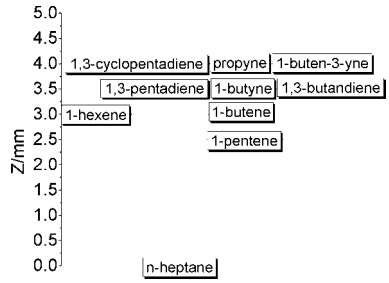

Figure 9. Peak position of hydrocarbon intermediates in flame A.

able to reveal the effect of oxygenate addition on the fuel decomposition and hydrocarbon growth processes. From this work, it is suggested that current *n*-heptane models with oxygenate addition need to include detailed chemistry that describes alkane decomposition to alkenes, such as pentene and butene, and the further decomposition of these alkenes to benzene precursors, such as butenynyl, butadienyl, and propargyl radicals.

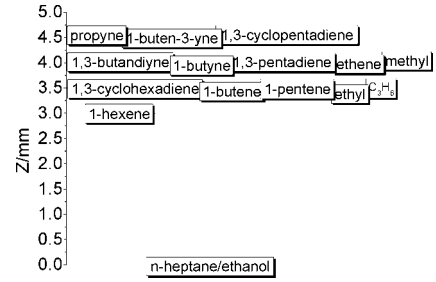

Figure 10. Peak position of hydrocarbon intermediates in flame B.

Acknowledgment. The authors acknowledge the financial support of the National Natural Science Foundation of China (50676065, 50576064, and 20533040). We also thank Prof. Adorina for her English revision. Furthermore, we appreciate the reviewers for constructive suggestions.

Supporting Information Available: Detailed data of each figure. This material is available free of charge via the Internet at http://pubs.acs.org.

EF800519S

(23) Leung, K. M.; Lindstedt, R. P. *Combust. Flame* **1995**, *102*, 129–160.
(24) Wang, H.; Frenklach, M. *Combust. Flame* **1997**, *110*, 173–221.
(25) Linstrom, P. J.; Mallard, W. G. *NIST Chemistry Webbook*; National Institute of Standards and Technology: Gaithersburg, MD, 2005.